
Composite Coatings for Fibre Bragg Grating Sensor in High Temperature Environments

Ying Huang^{1,*}, Fardad Azarmi², Mehdi Salimi Jazi²

¹Department of Civil and Environmental Engineering, North Dakota State University, Fargo, United States

²Department of Mechanical Engineering, North Dakota State University, Fargo, U.S.A

Email address:

ying.huang@ndsu.edu (Y. Huang)

To cite this article:

Ying Huang, Fardad Azarmi, Mehdi Salimi Jazi. Composite Coatings for Fibre Bragg Grating Sensor in High Temperature Environments. *International Journal of Sensors and Sensor Networks*. Vol. 3, No. 2, 2015, pp. 12-17. doi: 10.11648/j.ijssn.20150302.11

Abstract: Fiber Bragg grating (FBG) sensor has been widely applied for structural health monitoring of various applications due to its unique advantages of compact size, remote interrogation, electromagnetic hardening, high sensitivity, passive operation, real-time, and distributed sensing. However, the regular FBG sensors have a limitation of working below temperature of 300°C and without special care or expensive special sensor design, its use in high temperature environments is limited. In this paper, cost-effective composite coatings are developed to enable the use of FBG sensors in high temperature environments. The developed composite coatings combine various metal and nonmetal layers to achieve the best temperature elimination effects with less heat residual stress. The design of the composite coating is guided through theoretical and numerical modeling analysis of heat transfer and thermal stress progressing. Experimental studies have proved that the developed composite coating can work effectively to insulate heat effect for sensors up to 650°C without inducing significant deformation on the top of sensor surface from heat. The developed composite coating packaged FBG sensors, thus, may be able to apply for high temperature environments on a spacecraft in harsh service environments and buildings in fire environments.

Keywords: Composite Coating, Fiber Optic Sensors, High Temperature Environments, Structural Health Monitoring

1. Introduction

Structural health monitoring (SHM) has gained extensive attentions from engineering fields and it has been successfully applied to various engineering applications, such as civil, industrial, electrical, and aerospace engineering, etc. By collecting data from sensors on structures, a SHM system can track the health condition of a structure, which could allow the users to facilitate the adequate maintenance in advance to avoid system failure. To obtain the data for a SHM system, various sensors can be applied such as electrical, magnetic, acoustic, and optical fiber sensors [1], etc. Among these various sensors, fiber Bragg grating (FBG) sensor has been popularly applied in a SHM system due to its unique advantages of compact size, remote interrogation, electromagnetic hardening, high sensitivity, passive operation, real-time, and distributed sensing [2].

The FBGs are made by laterally exposing the core of a single-mode fiber to a periodic pattern of intense ultraviolet (UV) light, which creates a fixed refractive index modulation, called grating. At each periodic refraction change, a small amount of light is reflected, forming a coherent large

reflection at a particular wavelength known as the Bragg wavelength. Light signals at wavelengths other than the Bragg wavelength propagate through the grating with negligible attenuation or signal variation. The ability to accurately preset and maintain the grating wavelength is a fundamental feature and advantage of fiber Bragg gratings [3, 4]. Although FBGs can maintain permanent refractive index modulation in the fiber core, the performance of a FBG sensor is still significantly dependent on its working environments. The FBG sensors, either for strain, temperature, vibration, or chemical sensing, have very restricted requirements for the sensors' operational conditions. Exposure to high temperature environments usually results in the bleach of the refractive index modulation, limiting its temperature environment to be of less than 300°C [4].

Tremendous research efforts have been devoted to the development of high-temperature-resistant FBG sensors [5-10]. Using high peak power UV lasers, high reflectivity gratings known as Type II grating can be inscribed, which can work to temperature over 1,000°C [5, 6]. Ultrahigh peak power radiation generated by femtosecond pulse duration infrared (fs-IR) laser system [7] can also be used to fabricate

high temperature resistant grating [8]. If silica based fibers are used to fabricate the fs-IR generated grating, it can work temperature up to 1,000°C and if sapphire fibers are used, it can work above 1,750°C [9]. High temperature FBG sensor can also be doped using hydrogen-loaded germanium to resist temperature up to 1,000°C [10]. However, with these special design requirements, the fabrication of these high – temperature - resistant FBG sensors are very complex and costly, limiting their wide application for SHM of large-scale structures.

In addition to special fabrication of FBG sensors to resist high temperature, metal and non-metal coatings in single or multiple layers have been investigated as well for environmental protection for FBG sensors. Metal layers would increase the sensitivity of the sensor in extreme temperature. At the same time, metal coatings also reduce the sensor exposure to oxygen at extreme temperature, resulting in enhancement on environmental robustness. For instance, metal coatings with single layer of Al [11], Ni, Ag [12], and Au [13] have been investigated for high temperature environments up to 700 °C (973 °K). One single layer of non-metal coatings such as carbon fiber [14] and ceramic powders, though not popular as metal coatings, have also been investigated. One single coating on the top of the sensor would enhance the durability of the sensor in extreme temperature environments. However, the single layer coating will cause a thermal, thus, stress concentration within the coating. The resulted stress concentration will bring up micro or macro cracks inside the coating [12] and further alter the sensor's function and properties. Consequently, multilayer composite coatings which could reduce the thermal stress concentration in layers and retain the accurate sensing property of the sensors are needed.

On the other hand, cost-effective multiple-layer coatings with capability to resist high temperature environments such as fire are very popular in buildings, bridges, and aerospace engineering [15] for structural protection. However, limited studies consider to use cost-effective coatings to protect the FBG sensors from high temperature environments. Thus, it will be superior if innovative cost-effective coatings can be developed to enable the FBG sensors' capability to apply in high temperature environment. In this study, composite coatings are developed for FBG sensors to apply in high temperature environments. Theoretic and simulation model are developed to design the coatings followed by laboratory experiments to validate the effectiveness of the developed composite coatings in high temperature environments.

2. Theoretical Analysis of the Composite Coating

2.1. Theoretical Analysis Using Heat Transfer Theory

Heat transfer analysis is adopted to analyze the behavior of a multi-layer composite coating for FBG sensors in high temperature environments. Figure 1 shows an example layout of a three-layer structure of a composite coating, which has the

thermal conductivity of each layer of materials to be k_1 , k_2 , and k_3 , respectively. It is assumed during the analysis, no internal heat is generated, the system is isolated (no heat loss), and the heat flows at each layer are equal. For a three layer composite material, we have [16, 17]:

$$\frac{k_2(T_2-T_3)}{\Delta x_2} = \frac{k_1(T_1-T_2)}{\Delta x_1} \text{ and } \frac{k_2(T_2-T_3)}{\Delta x_2} = \frac{k_3(T_3-T_4)}{\Delta x_3} \quad (1)$$

where, T_1 , T_2 , T_3 , and T_4 are the temperature at each boundary between material 1, 2, and 3, and Δx_1 , Δx_2 , and Δx_3 are the thickness of each layer of the composite.

The thermal conductivity of the second layer of the composite can then be determined as follows:

$$k_2 = \frac{\Delta x_2 \cdot k_1 (T_1 - T_2)}{\Delta x_1 (T_2 - T_3)} \text{ or } k_2 = \frac{\Delta x_2 \cdot k_3 (T_3 - T_4)}{\Delta x_3 (T_3 - T_2)} \quad (2)$$

Thus, if the temperatures at the boundary of each layer, the thermal conductivity and thickness of the surface material of the spacecraft (k_1), and the thermal conductivity of the space (vacuum, k_3) are known, the thermal conductivity and thickness of the composite coating to be developed can be theoretically estimated and designed using Equation (2). For composites with more layers than three, the same theory can apply.

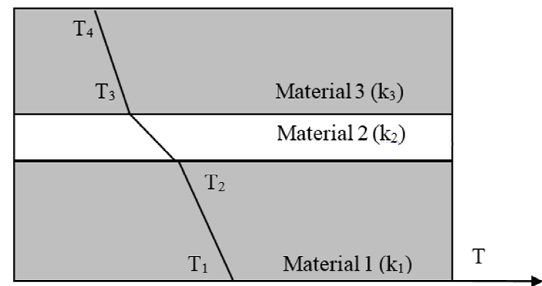


Figure 1. Layout of the three-layer composite.

2.2. Numerical Simulations

To apply the theoretic analysis, numerical simulations using commercial finite element modeling software ANSYS was performed to design the appropriate composite coating. The design started from a selection of a four-layer composite material with different thermal conductivity but same thickness (0.5 mm). Figure 2 shows the thermal conductivity of each layer and temperature boundary condition. An epoxy layer is required to attach the surface sensor which will be located the bottom layer of the composite. Two metallic layers using aluminum and NiCr were applied for initial analysis. In between the two metallic layers, one random layer of material with assumed thermal conductivity of 0.5 W/m.K was applied. The temperature at the outer layer of the coating which is assumed to be 1,200°C ($T_{out}=1,200^\circ\text{C}$), and the temperature required on the surface sensor of the spacecraft is assumed to be at room temperature of 25°C ($T_{in}=25^\circ\text{C}$) so that regular sensors can work appropriately.

Figure 3 shows the simulation results of the temperature variation through the composite coating. It can be seen that when a material with thermal conductivity less than 0.5

W/m.K was used in the third layer of the composite, the heat transfer reduced significantly from 1,200 °C to less than 700 °C. Aluminum as an intimate layer did not contribute to the heat reduction, resulting in a massive heat transfer to the epoxy layer. The predicted temperature on top of the epoxy was around 600 °C. The numerical simulation suggested that the aluminum must be replaced with a materials with less thermal conductivity and an epoxy with better high temperature resistant must be selected.

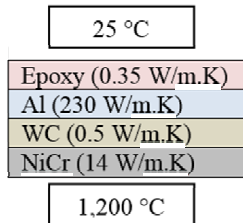


Figure 2. Four layer composite layout.

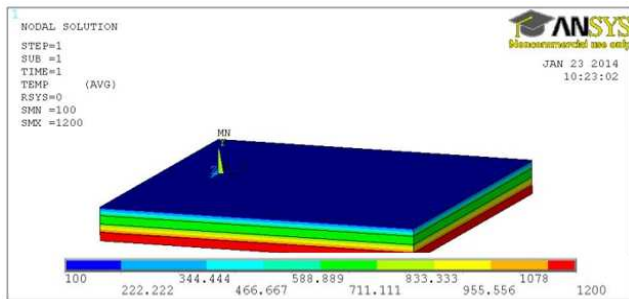


Figure 3. Heat distributions through the four-layer structure.

To improve the behavior of the composite coating under high temperature environments, the materials of the four-layer composite was re-selected. High temperature resistant epoxy was applied instead of regular epoxy. The aluminum layer was removed and the ceramic material was used as the WC layer. The NiCr layer was replaced by Inconel alloy together with high temperature epoxy. Figure 4 shows the layout of the multiple layer structure of the modified composite coating. The green bar between top steel and high temperature epoxy indicated the location of sensor. Each layer has a thickness of 0.5mm for the high temperature epoxy (Resbond 940 LE) and 0.8mm for the ceramic band. Inconel alloy 625 has been used as outer layer. The actual thermal conductivity and thickness of each layer is tabulated in Table 1. The thick steel layer on

top was used to avoid setting room temperature on the top of sensor and provide a gradual heat transfer.

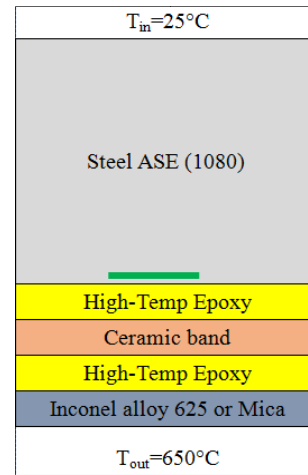


Figure 4. Modified four-layer composite layout.

Figures 5 shows the simulated heat transfer through the composite layout shown in Figure 4. The temperatures in contact with heater and top steel layer (T_{out} and T_{in}) were set at 650°C and 25°C, respectively. The ceramic band contributes significantly to the heat prevention through the composite. The composite successfully reduces the temperature from 650 °C to approximately 97 °C through the composite coating of 2mm in thickness.

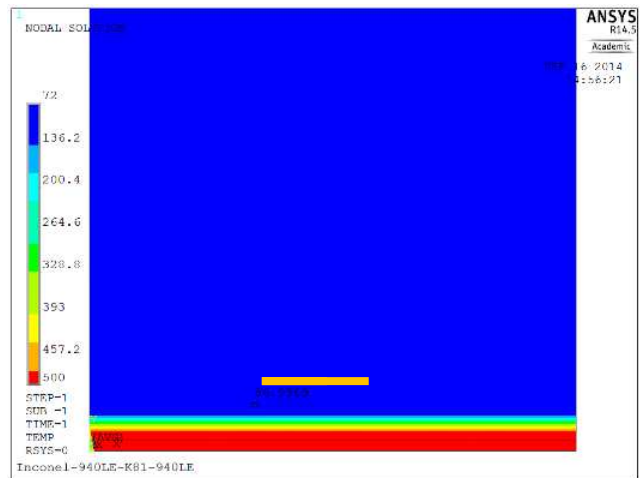


Figure 5. Simulated heat transfer through the five-layer structure.

Table 1. Material thermal conductivity.

Steel ASE (1080)		Inconel alloy 650		Ceramic band (87575K81)		High-temp epoxy	
Temp °C	W/m.°C	Temp °C	W/m.°C	Temp °C	W/m.°C	Temp °C	W/m.°C
127	56.7	93	10.8	260	0.055		0.721
327	48	204	12.5	534	0.087		
527	39.2	316	14.1	816	0.13		
727	30	427	15.7	1093	0.19		
		538	17.5				
		649	19				
		760	20.8				
		871	22.8				
		892	25.2				
Thickness (mm)	50	0.5		0.79 (0.8)		0.5	

3. Experiments and Discussion

3.1. Validation of the Composite Coating

To validate the design of the composite coating, one sample using the composite layer layout as shown in Figure 4 was constructed and high temperature experiments were conducted. Figure 6 (a) shows the experimental setup for temperature measurement of the sample. A heat plate was used to provide the high temperature environment on the bottom of the apparatus up to 650°C. One steel block was placed on bottom and top of the sample to form a uniform heat transfer. The height of the each steel block was 18.9 mm. Four thermal couplers (thermo-coupler K type) were placed, one on top of the hot plate, one on top and bottom of the test sample, and one above the top steel block. The sample was isolated from environments using thermal insulation material as shown in Figure 6 (b). A water-cooling system was applied to provide the desired room temperature environment on the top of the test sample.

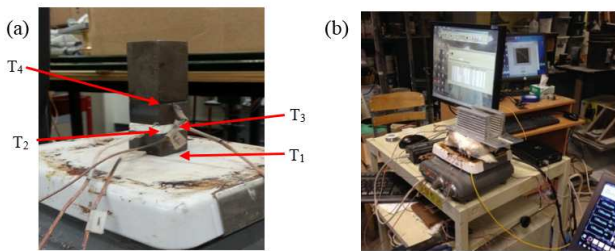


Figure 6. Experimental test set-up for (a) temperature sensor layout and (b) test setup.

The temperature with time was recorded at each interface and presented in Figure 7. With cooling on top of the steel block to simulate a room temperature of the inside surface of the spacecraft, the water cooler successfully reduced the temperature on the top of the sample to be around 100 °C. The developed composite coating successfully reduced the heat by 80%, approving an effective development of the insulation.

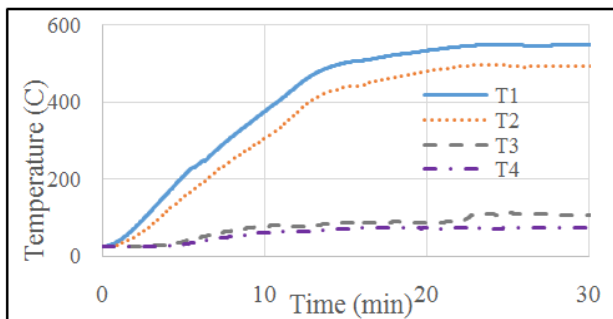


Figure 7. Variation of temperature at each layer.

From Figure 5, it can be seen that the temperature on top of the developed composite coating was calculated as 97 °C from the simulation. From Figure 7, it can be seen that the temperature at the same location was measured as 107 °C

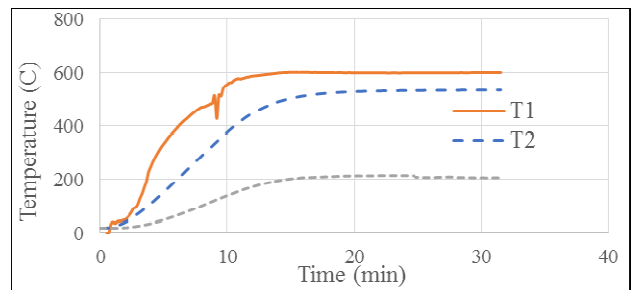
from the experimental test. The experimental results agreed well with the numerical simulation with relative error of less than 10%. Thus, the numerical simulations were effective and accurate to predict temperature distribution through developed composites. Upon validation, the results from the simulation could be further applied for material selections in high or low temperatures effectively.

3.2. Validation of the Coated FBG Sensors in High Temperature Environments

To validate the effectiveness of the developed composite coating for protecting FBG sensors from high temperature environments, another sample using the same materials in last section with a size of 2mm was fabricated with two types of sensors attached on the top of the sample. Figure 8 (a) shows the attached FBG sensor. Figure 8 (b) shows the detail measured temperature distributions along the test sample from the thermal couplers. A heat reduction of 65% was observed by using a water cooled system and proper insulation.



(a)

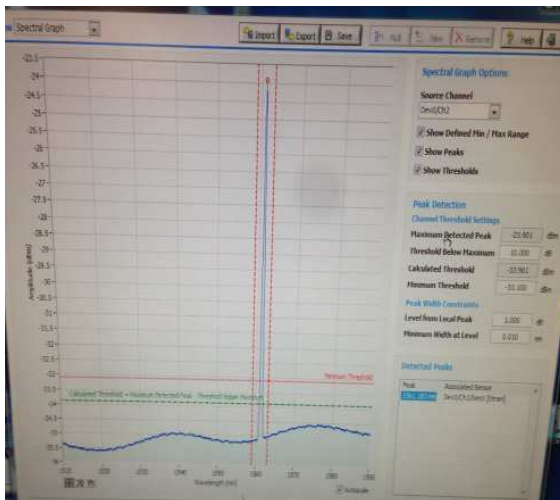


(b)

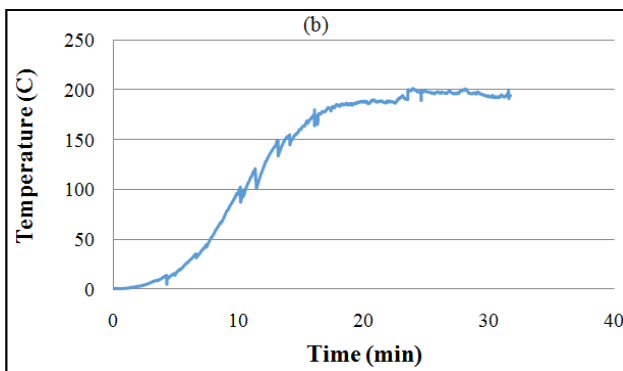
Figure 8. (a) Sample layout and (b) Temperature variances for the sensing test.

With a temperature of more than 200°C on the top of the test sample, electrical strain gauges are expected to be damaged, especially the wires to connect the sensors. Test results indicated the electrical strain gauges lost very quickly after the starting of the test. However, the fiber optic sensors, FBG sensors, were expected to work up to 300 °C. Figure 9 (a) illustrates screen shot of the spectrum detected by FBG sensor and Figure 9 (b) shows the measured temperature change by the FBG sensors with time. The test results indicated a successful survival of the FBG sensors through the high

temperature tests. The developed composite coating successfully protect the FBG sensors from damaging by the high temperature environments from the other side of the test sample.



(a)



(b)

Figure 9. (a) Screen-shot of example FBG sensor spectrum and (b) Temperature change measured by FBG sensor Vs time.

Table 2 compares the results obtained from embedded thermocouples and the FBG sensor. The relative variance between the two different measurements is around 2%, indicating an effective monitoring system using FBG sensors for temperature measurement.

Table 2. Comparison between results obtained from thermocouple and FBG sensor on top of the test sample.

	Thermo-coupler (°C)	FBG sensor (°C)	Relative variance
Temperature	206.5	202.3	2%

Upon various laboratory validation tests described above, the developed composite coating was capable of providing effective protection for fiber optic sensors in high temperature environments. The coated FBG sensors were approved to be accurate for measuring temperatures when they are in a low range. With the protection from the developed composite coatings, these sensors could apply to higher temperature service condition for both temperature and strain/stress sensing.

4. Conclusions and Future Work

In this paper, a theoretic and simulation model was developed to design innovative multilayer composite coatings for FBG sensors in high temperatures. A four-layer composite with both metal and non-metal materials was developed and numerical simulation approved the effectiveness of this composite for temperature up to 600 °C. Laboratory tests were performed to validate the simulation and a relative error of less than 10% was observed, which indicating an effective model for the composite design analysis. The developed composite coating was used to protect a FBG sensor in laboratory. The experimental results approved a 65% of heat reduction by using the developed coating and the survival of the sensor under such a high temperature environment of 600 °C. In the near future, higher temperature will be tested and the structural behavior of the developed insulation will be investigated as well.

Acknowledgements

Financial support to complete this study was provided by the ND NASA EPSCoR under Agreement No.FAR0021960 and U.S. DOT PHMSA under Agreement No. DTPH56-13-H-CAAP05. The findings and opinions expressed in the paper are those of the authors only and do not necessarily reflect the views of the sponsors.

References

- [1] H. Sohn, C. R. Farrar, F. M. Hemez, D. D. Shunk, D. W. Stinemat, B. R. Nadler, and J. J. Czarnicki, "A Review of Structural Health Monitoring Literature: 1996–2001," Los Alamos National Laboratory Report, LA-13976-MS, 2004.
- [2] E. Udd, *Fibre Optic Sensors*, John Wiley and Sons: New York, NY, 1999.
- [3] F. T. S. Yu and S. Yin, *Fiber optic sensors*, New York: Dekker, 2002, Chaps. 2 and 4 and p. 124.
- [4] S. J. Mihailov, "Fiber Bragg Grating Sensors for Harsh Environments", *Sensors*, Vol. 12, pp. 1898-1918, 2012.
- [5] J. L. Archambault, L. Reekie, and P. S. J. Russell, "High reflectivity and narrow bandwidth fibre gratings written by single excimer pulse", *Electron. Lett.* Vol. 29, pp. 28-29, 1993.
- [6] C. G. Askins, M. A. Putman, G. M. Williams, and E. J. Friebele, "Stepped wavelength optical fiber Bragg grating arrays fabricated in line on a draw tower," *Opt. Lett.*, Vol. 19, pp. 147-1479, 1994.
- [7] K. M. Davis, K. Miura, N. Sugimoto, and K. Hirao, "Writing waveguides in glass with a femtosecond laser," *Opt. Lett.*, Vol. 21, pp. 1729-1731, 1996.
- [8] S. J. Mihailov, D. Grobncic, C. W. Smelser, P. Lu, R. B. Walker, and H. Ding, "Bragg grating inscription in various optical fibers with femtosecond infrared lasers and a phase mask," *Opt. Mater. Exp.*, Vol. 1, pp. 754-765, 2011.

- [9] D. Grobnic, S. J. Mihailov, C. W. Smelser, and H. Ding, "Sapphire fiber Bragg grating sensor made using femtosecond laser radiation for ultrahigh temperature applications," *IEEE Photon. Technol. Lett.*, Vol. 16, pp. 2505-2507, 2004.
- [10] B. Zhang and M. Kahrizi, "High-Temperature Resistance Fiber Bragg Grating Temperature Sensor Fabrication," *Sensors Journal*, IEEE, Vol. 7, No. 2, pp. 586- 591, 2007.
- [11] R. Rajini-Kumar, M. Suesser, K. G. Narayankhedkar, G. Krieg, and M. D. Atrey, "Performance Evaluation of Metal-coated Fiber Bragg Grating Sensors for Sensing Cryogenic Temperature", *Cryogenics*, Vol. 48, pp. 142-147, 2008.
- [12] X. Zhang, *Sensitivity Alteration of Fiber Bragg Grating Sensors through On-fiber Metallic Coatings Produced by A Combined Laser-assisted Maskless Microdeposition and Electroless Plating Process*, Master Thesis, the University of Waterloo, 2013.
- [13] A. Méndez and T. F. Morse, *Specialty Optical Fibers Handbook*, Elsevier Academic Press: San Diego, CA, 2007.
- [14] C. Holton, "Protected High Temperature Optical Fiber Sensors, Gauge Elements and Systems", in *Fundamental Aero Program Workshop*, New Orleans, 2007.
- [15] M. M. Finckenor and D. Dooling, "Multilayer Insulation Material Guidelines", NASA STI office, Report No. NASA/TP-1999-209263, April 1999.
- [16] J. P. Holman, *Heat Transfer*, 10th edition, McGraw-Hill Publishing Company: New York, NY, 2009.
- [17] G. M. Armando, V. C. Christian, A. B. B. José, H. R. H. Víctor and M. B. F. José, *Analysis of the Conjugate Heat Transfer in a Multi-Layer Wall including an Air Layer*, Chapter 22 in *Heat Transfer - Mathematical Modelling, Numerical Methods and Information Technology*, InTech: Rijeka, Croatia, 201.